Challenges and opportunities in high efficiency scalable and stable perovskite solar cells

Cite as: Appl. Phys. Lett. **125**, 170501 (2024); doi: 10.1063/5.0232621
Submitted: 9 August 2024 · Accepted: 8 October 2024 ·
Published Online: 21 October 2024

Kashimul Hossain, Suryanarayan Nayak, and Dinesh Kabra[a)]

AFFILIATIONS

Department of Physics, Indian Institute of Technology Bombay, Powai, Mumbai 400076, India

[a)]Author to whom correspondence should be addressed: dkabra@iitb.ac.in

ABSTRACT

Perovskite solar cells (PSCs) are the fastest-growing photovoltaic (PV) technology and hold great promise for the photovoltaic industry due to their low-cost fabrication and excellent efficiency. To achieve commercial readiness level, the most important factor would be yield beyond 95% at the PSC module levels. The current essential requirements for PSCs are reproducibility of high efficiency devices, scalability, and stability. The reported certified high efficiency (24–26%) results are based on the use of $FAPbI_3$ perovskites with a bandgap of $E_g \approx 1.5$ eV, and the typical device's active area ranges from ≈ 0.1 cm^2 to a maximum of 1 cm^2. However, relatively higher bandgap PSCs are essential, especially in tandem solar cell applications. Hence, optimization of higher bandgap PSCs is a necessity. As the bandgap of the perovskites increases, the efficiency goes down due to reduced J_{SC} and increased V_{OC} loss. Therefore, understanding the loss mechanism and corresponding solutions need to be developed. Scaling up the device's active area without compromising the fill factor and, hence, efficiency is nontrivial. So, understanding the loss mechanism in large area devices is crucial. The stability analysis reported in the literature is inconsistent, preventing data comparison and identifying various degradation factors or failure mechanisms. Moreover, how the accelerated tests would be useful in predicting the real lifetime of the solar cells is yet to be developed. So, understanding the knowledge and the technological gaps between laboratory and industry-scale production is crucial for further development. Therefore, in this review article, we discuss the challenges and opportunities for scalable and stable high efficiency PSCs.

I. INTRODUCTION

The journey of perovskite solar cells (PSCs) began with the concept of dye-sensitized solar cells (DSSCs) in the *n-i-p* (aka "regular") device architecture.[1] In 2009, Miyasaka *et al.* used hybrid organometallic halide perovskite $MAPbI_3$ in the DSSCs and achieved an efficiency of 3.81%.[1] Currently, the reported efficiency of the perovskite solar cells is ∼26% in both *n-i-p*[2] and *p-i-n* (aka "inverted")[3] device architectures, where the practical achievable limit[4] could be ∼30%. The *p-i-n* device architecture has several advantages, including low-temperature processability of the charge transport layers (CTLs) and long-term operational stability derived from non-doped hole transport layers.[5] In addition, the *p-i-n* architecture-based device is crucial in monolithic tandem solar cells such as perovskite–perovskite, perovskite–organic, and perovskite–CdTe (except Si–perovskite) tandem solar cells.[6] Such a speedy journey[1–3] of efficiency improvement of the perovskite solar cells (PSCs), i.e., 3.81% to ∼26% could be accredited to the unique optoelectronic features of perovskites such as high absorption coefficient, low exciton binding energy, long diffusion length, tunable bandgap, etc.[7–10] As expected, the polycrystalline perovskites form shallow defects within the bandgap, and this defect density decreases rapidly as energy increases from the band edge toward the mid-gap.[11] However, different passivation engineering strategies are employed to minimize the interface and bulk defect states and improve the efficiency and stability of perovskite solar cells.[12] To commercialize the perovskite solar cells, the essential requirements are (i) highly reproducible state-of-the-art efficiency, (ii) cost-effective scalable device production, and (iii) improved device lifetime.[13] Until now, researchers have mainly focused on the enhancement of efficiency in the dot (area < 1 cm^2) perovskite solar cells[14] and achieved efficiency close to the market leading c-silicon solar cells (∼27%).[1–3] Nevertheless, despite having high efficiency values on lab-scale PSC devices (<1 cm^2), the current bottleneck is the scalability and stability, which affects the levelized cost of energy (LCOE). The LCOE is a techno-economical term that is being used to evaluate the cost of energy production rate considering the material cost, fabrication cost, efficiency of the cell, lifetime of the cell, etc. The levelized cost of energy is defined as

$$LCOE = \frac{sum\ of\ costs\ over\ lifetime}{sum\ of\ the\ energy\ produced\ over\ lifetime}.$$

Recently, it is shown that the LCOE of the PSCs varies from 3 to 6 US cents per kWh^{-1}, whereas for the Si solar cell, the LCOE decreased from \$76 to 30 US cents in 2015 and is almost saturated. The LCOE of PSCs could be further reduced by enhancing the device's scalable production rate and lifetime. Therefore, a deep understanding of the challenges and corresponding solutions needs to be discussed. Initially, the physical and optical properties of the $MAPbI_3$ perovskite (bandgap ~1.6 eV) are widely explored, but interestingly and reassuringly, the reported high efficiency observed in the $FAPbI_3$ (with additive/interface engineering) perovskite absorber of bandgap ~1.5 eV.[2,3] Apart from efficiency, the $FAPbI_3$ perovskite is thermally more stable than the $MAPbI_3$ perovskite.[15,16] Furthermore, Saliba *et al.* incorporated Cs to improve the thermal stability of Methylammonium Formamidinium (MAFA) halide-based perovskite crystal structure and the resulting bandgap of ~1.60 eV.[17] Hagfeldt *et al.* showed a detailed roadmap of the evolution of perovskite's compositional and interface engineering strategy for the efficient and stable device fabrication.[18] However, a slightly wide-bandgap perovskite absorber ($\gtrsim$ 1.65 eV) has become popular due to their use in tandem solar cells such as perovskite–perovskite,[19] perovskite–Si,[6] perovskite–CdTe,[20] etc. The efficiency is compromised in the wide bandgap perovskite solar cells due to loss in the J_{SC} because of absorption spectrum loss and V_{OC} loss because of non-radiative trap states or band alignment mismatch. Although the loss in the spectrum is not a problem for the wide bandgap perovskites in tandem architecture, but V_{OC} loss is a serious concern. Therefore, understanding the V_{OC} loss mechanism and corresponding solutions need to be discussed, which would be beneficial in single-junction and tandem solar cells. Apart from that the scalability of the PSC while maintaining the efficiency is challenging. Literature study indicates that as the active area of the devices increases the efficiency compromises; however, the specific photovoltaic (PV) parameter that has the most significant impact is not elaborated yet. Recently, several groups tried different device engineering on high efficiency (~25%) PSCs and increased the active area from 0.1 to 1 cm^2.[2,3,21–23] These areas are still much smaller compared to the commercialized silicon solar cell (M6) device area. However, the observed fact is that the efficiency of the slightly higher device area (1 cm^2) is no longer same compared to the 0.1 cm^2. Even though, mini-module of the perovskite solar cells is being introduced, the efficiency is significantly compromised.[24] Therefore, it raises a serious concern whether the perovskite PV technology would be able to be commercialized or not. The challenging factors in upscaling the device active area of PSCs need to be discussed. Moreover, the stability reported in the literature is inconsistent and prevents data comparison. So, identifying the various degradation factors and failure mechanisms would be difficult to correlate. Interestingly, unlike other PV technology, perovskite degradation is known to be reversible partly or entirely in the dark.[25] Therefore, how the indoor ISOS (International Summit of Organic PV Stability) stability test protocols using constant 1-sun illumination would be useful in predicting the real field lifetime for PSCs is not known. Several groups reported PSCs stability at MPPT (maximum power point tracking) and constant illumination under 1-sun condition, and it shows $T_{90} > 1000$ h.[26] This stability indicates the potential of PSCs toward commercialization, but how these accelerated tests would be useful in predicting the practical lifetime of the solar cells is not well understood. As a matter of fact, several research groups and industries are working to solve these issues. The cost-effective production of energy from the PSCs has grabbed much attention in the solar cell community, and companies like Microquanta Semiconductor (China), RenShine Solar (China), Kunshan GCL (China), Hanwha Q CELLS (South Korea), Oxford PV (UK and Germany), and so on are involved in R&D, aiming for commercialization of perovskite solar cells in single-junction and tandem device architectures. Microquanta demonstrated 20.2% efficiency on 20 cm^2 solar cell area and 14.24% efficiency for large-area (200 cm × 800 cm) solar modules.[27] RenShine Solar achieved a certified efficiency of 19.42% on a 30 cm × 40 cm perovskite solar module and passed the IEC61215 reliability tests.[28] Kunshan GCL showed an efficiency of 19.04% on the single-junction perovskite module of area 100 cm × 200 cm, aiming for the world's first large-scale 2 GW perovskite production line.[29] However, these recipes are not available in the public domain. Evidently, further progress is required to minimize the levelized cost of energy (LCOE) for commercialization of perovskite solar cells.[30] To throw more light on this area, here, we discuss the challenges and opportunities to have scalable and stable high efficiency perovskite solar cells.

II. BANDGAP TUNING AND EFFICIENCY LIMITATION

Perovskite is a class of semiconducting materials with a crystal structure of ABX_3, where A and B are the positively charged atoms/molecules of different sizes, and X is the halide. Figure 1(a) represents the schematic of the typical crystal structure where the black ball at the center of the crystal represents the monovalent A cations (Cs^+, FA^+, and MA^+), the blue balls at the center of each octahedral represent the divalent B cations (Pb^{2+} and Sn^{2+}) and the red balls at the corner of the octahedral indicate X halides (I^-, Br^-, and Cl^-).[31] Initially, the physical and optical properties were widely explored for the $MAPbI_3$ and $FAPbI_3$ perovskites. However, mixed organic–inorganic halide perovskites came into the picture later with different bandgaps. Interestingly, the bandgap of tin-lead mixed perovskite is 1.2–1.3 eV, i.e., lower than the tin- and lead-based perovskite due to the bowing effect, and it is close to the ideal Shockley–Queisser (SQ) limit bandgap in single-junction solar cells, whose efficiency could be ~33%. Despite being an ideal bandgap, the efficiency is still lower than the lead-based PSCs and suffers from stability issues as Sn^{2+} is easily oxidized to Sn^{4+}, causing p-type self-doping and forming Sn vacancies as recombination centers.[32] Figure 1(b) shows that the bandgap of the perovskites can be tuned from 1.2 to 3.7 eV by adjusting the ratios of A-cite cation (cesium: Cs; methylammonium: MA; formamidinium: FA), B-cite cation (lead: Pb; Tin: Sn), and halides (iodine: I; bromine: Br; chlorine: Cl).[32] The first-principles calculation indicates that the formation energy of the intrinsic point defects (vacancy, interstitial, anti-sites, etc.) could be maximized by mixing different A-cite cations,[33] and thermodynamic stability enhanced by halides mixing[34] to a certain ratio. The mixed halide wide bandgap (>1.65 eV) perovskites have become popular due to their use in tandem solar cell applications. The tandem solar cells comprise different bandgap semiconductors in a single-junction device and can overcome the efficiency limit of single-junction solar cells by minimizing the below bandgap loss and thermalization loss. The detailed balance study under standard conditions (AM 1.5 G spectrum, 1000 W/m^2, 25 °C) shows the efficiency limit[35] of a single-junction solar cell to be 33.77% for a semiconductor of bandgap 1.34 eV, whereas the two terminal (2 T) tandem cells of Si/perovskites could reach efficiency up to ~46% by using the Si solar cell

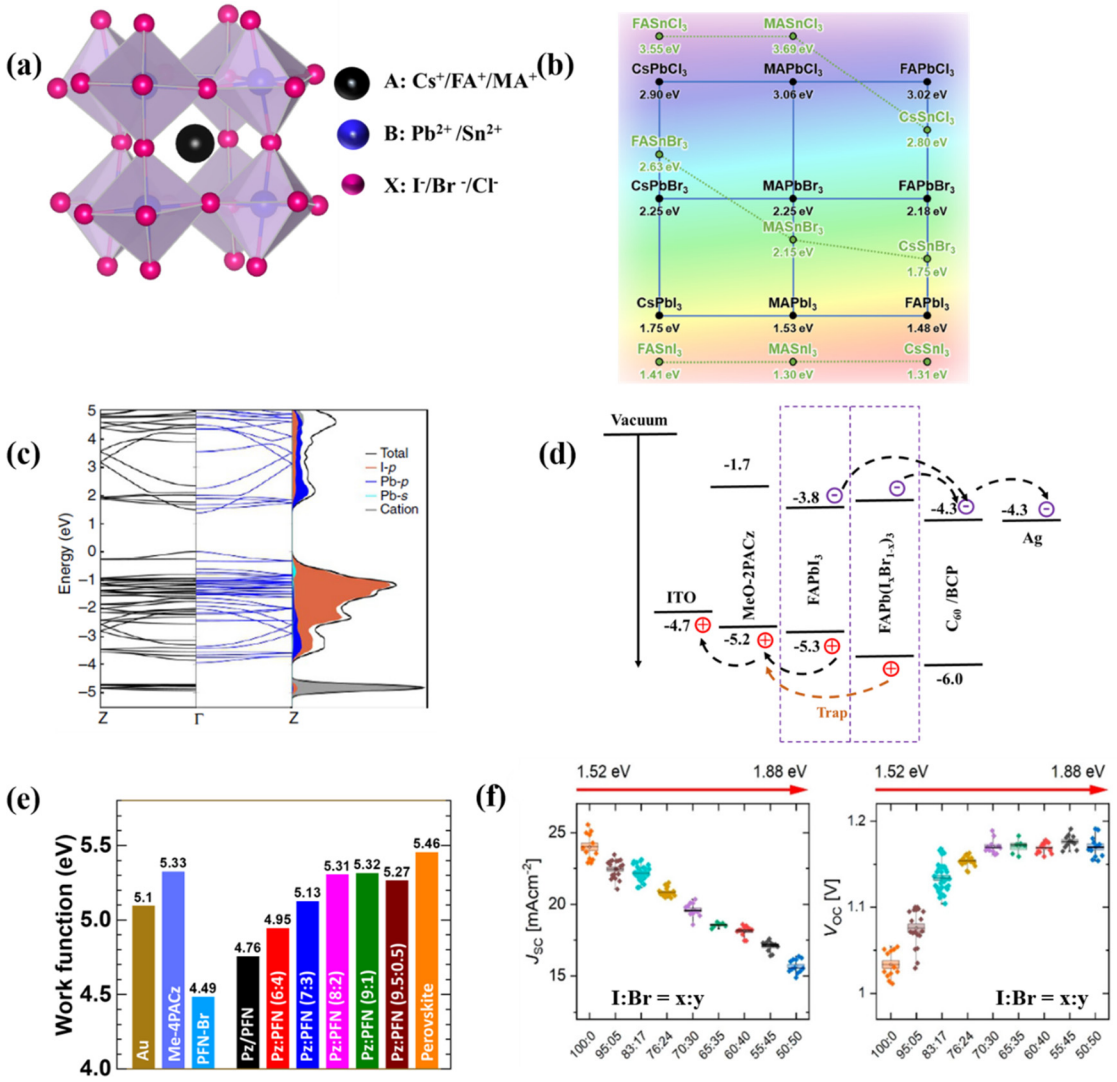

FIG. 1. (a) Schematic of the ABX_3 organic–inorganic metal halide perovskite crystal structure. (b) Bandgap energy of ABX_3 perovskites. Reprinted with permission from Seo *et al.* Adv. Energy Sustainable Res. **4**, 2200160 (2023). Copyright 2023 Wiley-VCH.[32] (c) The electronic band structure and partial density of states (PDOS) of $MAPbI_3$ perovskites. Reprinted with permission from Flip *et al.* Nat. Commun. **5**(1), 5757 (2014). Copyright 2014 Springer Nature.[37] (d) Energy level band diagram of p-i-n architecture-based perovskite solar cells. The energy level values are taken from the literature.[5] (e) Work function of the HTL tuning for 1.6 eV bandgap perovskite solar cells. Reprinted with permission from Kabra *et al.* ACS Energy Lett. **8**, 3860 (2023). Copyright 2023, American Chemical Society.[41] (f) The current density (J_{SC}) and open circuit voltage (V_{OC}) variation as a function of I:Br = x:y mixing ratio (or varying bandgap). Reprinted with permission from Camargo *et al.* ACS Energy Lett. **5**, 2728 (2020). Copyright 2020, American Chemical Society.[42]

bandgap of 1.12 eV and PSC of bandgap 1.73 eV (at 25 °C).[36] It is important to note that the perovskite has a positive temperature coefficient and the bandgap increases with elevating temperature (>55 °C) during operation. Therefore, the optimum bandgap for the perovskite in Si/perovskite tandem solar cells is 1.68 eV (at 25 °C).[36] The perovskite − perovskite, perovskite–CdTe, perovskite − organic, and triple-junction tandem solar cells require further higher bandgap perovskite absorber to minimize thermalization loss. The wide bandgap (>1.65 eV) mixed halide perovskites (MHPs) suffer from phase segregation, especially when the Br:I concentration ratio is >25%, which leads to poor optoelectronic properties and stability.[36] The efficiency is lower in the wide bandgap perovskite solar cells due to J_{SC} loss (narrow absorption spectrum) and V_{OC} loss. Although the loss in the absorption spectrum (or J_{SC}) is not a problem for the wide bandgap perovskites in tandem architecture, V_{OC} loss is a serious concern. The loss in V_{OC} could be attributed to the non-radiative recombination within the bulk of the perovskite layer and at the interface of the perovskite/charge transfer layer (CTL). The bulk defects can be

minimized by improving the perovskite crystal quality (additive engineering and vapor deposition), but the interface issue requires attention in high bandgap perovskites. Figure 1(c) represents the electronic band structure and partial density of states (PDOS) of $MAPbI_3$ perovskites.[37] The electronic band structure of the mixed halide perovskites (MHPs) indicates that halide p-orbital states dominate the valence band maximum (VBM), and the conduction band minimum (CBM) is merely derived from the metal p-states. Therefore, to widen the bandgap, Br or Cl is incorporated into I-based perovskites and the valence band goes deeper into the energy level. The shift down of the VBM energy level (or slightly shift up of CBM) introduces band energy offset with the charge transport layer and results in difficulties in the charge carrier collection. Figure 1(d) represents the schematic of the $FAPbI_3$ ($E_g = 1.51$ eV) perovskite-based *p-i-n* architecture solar cell (energy levels values are taken from literature).[5] It is evident that the HOMO level of the hole transport layer (HTL) −5.2 eV is well matched with the VBM (−5.3 eV) of $FAPbI_3$ perovskite absorber and results in $V_{OC} \approx 1.2\,eV$.[5,38] The similar energy alignment is also observed in the high efficiency *n-i-p* device architecture, where the HOMO level of spiro-OMeTAD is well matched with the $FAPbI_3$ perovskite's VBM and results in $V_{OC} \approx 1.2\,eV$, i.e., with a voltage loss of ∼0.3 eV.[21] However, if the higher bandgap mixed halide perovskite is introduced in this *p-i-n* device architecture [Fig. 1(d)], the energy level alignment offset introduces difficulty in charge collection and leads to loss in V_{OC}.[39] Kirchartz *et al.* carried out interface optimization engineering using different ETLs (electron transport layers) for a 1.72 eV bandgap perovskites and obtained the highest $V_{OC} \approx 1.35$ V resulting loss in voltage of 0.37 V. Snaith *et al.* carried out surface passivation engineering using different combination of HTLs for 1.8 eV bandgap perovskite and achieved highest $V_{OC} \approx 1.29$ V resulting resulting loss in voltage of 0.51 V. Saliba *et al.* recently reported the highest V_{OC} of 1.78 V using $MAPbCl_3$-based perovskite of bandgap 3.03 eV in *n-i-p* device architecture with Spiro-OMeTAD as HTL, resulting in loss in voltage of 1.25 V.[40] Our group has also minimized the band offset between the HTL and perovskite ($E_g = 1.6$ eV) interface by modifying the HTL work function [see Fig. 1(e)].[41] The work function is measured using kelvin probe force microscopy (KPFM) study with gold as the reference work function (and verified with UPS study). It is clear that the work function of self-assembled monolayer (SAM) Me-4PACZ HTL is well matched with perovskites; however, the deposition of a uniform perovskite layer is difficult on pure a Me-4PACz layer due to hydrophobicity issue.[41] Therefore, PFN-Br is mixed with Me-4PACz in different volume ratios to resolve the hydrophobicity issue and deposit a uniform perovskite layer.[41] The Pz:PFN (9:1), which is a mixed composition of Me-4PACz and PFN:Br in 9:1 volume ratio, is the optimized composition for minimum band offset and showed efficiency >20% with $V_{OC} = 1.16$ eV. Camargo *et al.* studied $Cs_{0.05}(FA_xMA_{1-x})_{0.95}Pb(I_xBr_{1-x})_3$ perovskites where x varied from 0.5 to 1.0 and, correspondingly, the bandgap tuned from 1.5 eV to 1.9 eV.[42] They observed that the J_{SC} of the device decreases linearly with the bandgap (absorption spectrum loss), whereas the V_{OC} of the devices saturated at the higher bandgap [see Fig. 1(f)]. This loss in the V_{OC} could be related to the band offset of the HTL/perovskite interface because the same HTL cannot hold similar energy alignment with different bandgap (or VBM) perovskites. Jeong *et al.* showed that minimizing the offset in the band alignment of $FAPbI_3$ perovskite and HTL Spiro-OMeTAD by modifying it results in improvement in the V_{OC} and voltage loss as minimum as 0.3 V.[21] However recently, various deeper HOMO level-based self-assembled monolayer (SAM) HTLs grabbed significant attention in the wide bandgap perovskites due to better band energy alignment and faster charge transfer and showed improvement in V_{OC} and *FF*.[43]

The perovskite database[44] shows that $J_{SC}/J_{SC,SQ}$ of the devices are approaching unity for all bandgap perovskites, whereas $V_{OC}/V_{OC,SQ}$ is close to unity for narrow bandgap perovskites and is less than unity for the higher bandgap perovskites (subscript SQ indicates the Shockley–Queisser limit).[12] Cahen *et al.* also carried out the quantitative analysis of J_{SC} and V_{OC} loss in different bandgap perovskites and observed the similar results.[45] The literature study indicates that the lead (Pb)-based high efficiency (24%–26%) single-junction solar cells are still using lower bandgap (1.5 eV) $FAPbI_3$ perovskites because of good band energy alignment of the perovskite absorber with the available HTLs and observed a V_{OC} loss of as minimum as 0.3 V. As of now, the V_{OC} loss is mainly attributed to non-radiative defects in the bulk and at the interface, but band energy alignment issue is not well elaborated yet. Very recently, Wolf and coworkers tried to focus on this aspect by tailoring the SAM-based HTL's using mixing engineering strategy for perovskite absorbers of bandgap 1.69, 1.81, and 2.0 eV.[46] However, a systematic HTL/perovskite interface band offset study (experimental or simulation) is required and simultaneously deeper HOMO level-based HTLs needs to be developed to minimize the V_{OC} loss for wide bandgap PSCs. This study will likely to be helpful to minimize the V_{OC} loss and improve the FF of the wide bandgap PSCs, resulting in improvement in efficiency in the single-junction as well as tandem solar cells.

III. SCALABLE PEROVSKITE SOLAR CELLS AND EFFICIENCY LIMITATION

Solution-processed photovoltaic technologies grabbed much attention in the solar cell community and reported certified high efficiency (>25%) using $FAPbI_3$ (or ∼5% Cs added) perovskite absorber of bandgap ∼1.5 eV over the device active area of $\leq 0.1\,cm^2$.[38] It is evident that, in terms of lab-scale device efficiency, this value is competitive with established commercialized technologies. However, the perovskite community is still far from commercializing the perovskite photovoltaic technology as the efficiency is not similar in the slightly large area (1 cm^2) devices yet, regardless of the deposition techniques. In academic labs, people have demonstrated significant progress in PSCs over device active areas of up to 1 cm^2 and mini-modules. However, a few industries, e.g., Kunshan GCL, showed efficiency >19% on the single-junction perovskite module of area 2 m^2, but the information is not available in the public domain.[47] Therefore, researchers must focus on developing strategies for high performance scalable perovskite solar cells and perovskite module fabrication. Since this is a thin-film device technology with many layers being deposited via the solution route, it seems to be one of the major challenges in scaling up. Typical thicknesses of absorber layers in other established thin-film PV technologies like GaAS and CdTe are of 10–12 μm and 4–6 μm, respectively; however, in the case of PSCs, it is hardly 600–800 nm. Furthermore, both established thin-film PV technologies use typically vacuum-based deposition techniques (vacuum-transfer deposition for CdTe and MBE for GaAs PVs), whereas halide perovskite PV performance is typically processed via solution route. Vacuum-processed perovskite lags behind in terms of efficiency. At least in the academic laboratory, scaling up via the solution route is challenging.

Recently, we have demonstrated that the fabrication of large area PSCs by spin coating is challenging as the leakage current in the device increases exponentially, which may be due to non-uniform deposition of the perovskite layer in a multi-layered stack device.[48] However, different deposition techniques have been developed, such as vacuum processing (thermal evaporation and pulsed laser deposition) and solution processing (blade coating, spray coating, slot dye coating, inject printing, and screen printing) apart from the spin coating technique to make a uniform perovskite layer over large area substrates. Even though the blade coating and evaporation-based technique showed an efficiency of ~25% over a small area ($\leq$0.1 cm^2) device, the up-scaled perovskite solar modules (PSMs) of area ~100 cm^2 showed better efficiency (~18%) in evaporated devices due to conformal deposition over large area substrates. However, solution-based techniques such as spray coating, slot die coating, and inject printing-based devices have lower cell efficiency in small area cells (0.1 cm^2) but relatively improved efficiency performance in PSMs. Therefore, contrasting the photovoltaic performance with cell and module sizes of different deposition techniques makes it difficult to compare their performance disparities fairly and consistently. Chalkias *et al.* develop a mathematical equation to ascertain the scaling-up factor ($f_{scalling_up}$)[49,50] as

$$f = \frac{1 - \frac{\eta_{module}}{\eta_{cell}}}{\log\left(\frac{A_{module}}{A_{cell}}\right)} \times 100\%,$$

where η is the PCE, and A is the active area of the cell or module. The lower value of f indicates less scaling-up loss from PSCs to PSM, which is essential for commercialization. Interestingly, it is observed that f = 3.48% for the inject printing process (A_{cell} = 0.105 cm^2, A_{module} = 804 cm^2, η_{cell} = 20.7%, η_{module} = 17.9%) and f= 8.57% for the evaporation-based process (A_{cell} = 0.16 cm^2, A_{module} = 228 cm^2, η_{cell} = 24.8%, η_{module} = 18.1%), indicating the possible direction of scaling up the process in the future.[51] People have reported in various review papers that scaling up of the PSCs active area results in poor efficiency, but which PV parameter affects the most is not well elaborated. Additive and interface engineering were adopted to improve the efficiency over large area PSC devices, but the efficiency and reproducibility both decrease on increased device's active area, which restricts the PSCs toward commercialization.[52] Even though the PSC research started with the millimeter square device area, researchers have recently focused on taking it to the centimeter square device area. Deplorably, the literature study shows that there is a lack of representation of the performance of PSC in large areas. Many of the reported papers have demonstrated high efficiency PSC's performance but do not report the device area; we deliberately avoid to refer them here. However, we believe that this is an important parameter to be checked at all levels, i.e., authors, editors, and reviewers. Even some groups report the device's active area in the supplementary information file, which is a bad practice, and the reader needs to open another file to get the information on the device area. It would be good if the authors report the device's active area with dimension (length × width) in the main text along with the device image. Also, the sheet resistance of the transparent conductive oxide (TCO) substrate on which the device is fabricated could influence the device's performance; hence, it is important to mention the sheet resistance (Ω/Sq) of the substrates.[53] It is also important to include the list of materials, device characterization tools, and detailed information on characterization techniques. Saliba *et al.* studied 16 000 papers and showed that the short circuit current density (J_{SC}) measured from $J-V$ scans is 4%–5% higher than the J_{SC} measured from integrating the EQE spectrum.[54] This mismatch could be attributed to either edge effect[55] from the active area of the device or pre-bias measurement condition.[56] Some groups use a non-reflective metal mask aperture on the top of the active area during $J-V$ scans, which could avoid the edge effect.[38] Since the dimension of the aperture masks influences the PV parameters, such as V_{OC} and FF, it should be $\geq$ 80% of the device's active area.[57] Apart from that, recently, people reported excellent efficiency on the small area (<0.1 cm^2) and relatively larger area (1 cm^2) devices. However, they certify the efficiency on small area devices only or use an aperture mask of small

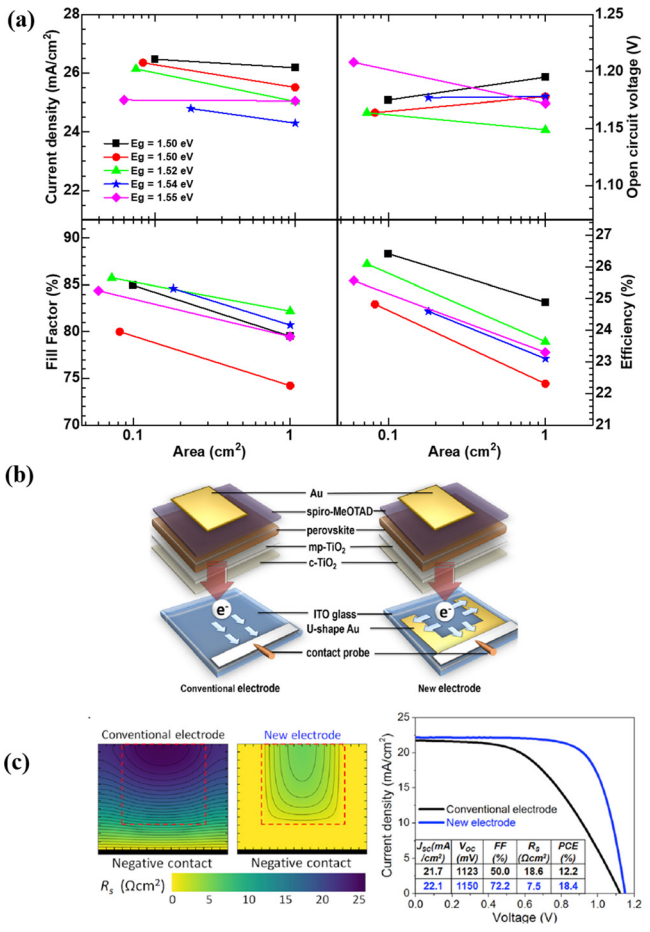

FIG. 2. (a) Photovoltaic (PV) parameters as a function of device active area for the highest efficiency reported perovskite solar cells (PSCs).[2,3,21–23] (b) 1-cm^2 active area n-i-p architecture-based PSC with the conventional electrode (left) and U-shaped new electrode design (right). Reprinted with permission from Ho-Baillie *et al.* Joule **2**, 2694 (2018). Copyright 2018 Elsevier Inc.[53] (c) Images on the left indicate the simulated series resistance distribution for the 10 × 10 mm^2 active area device (red dashed lines define active area), and the right panel $J-V$ characteristics show the performance comparison of the conventional and new electrode designed PSCs. Reprinted with permission from Ho-Baillie *et al.* Joule **2**, 2694 (2018). Copyright 2018 Elsevier Inc.[53]

area (<0.1 cm^2), and that results in lack of confidence in large area PSCs.[22] Figure 2(a) represents the reported high efficiency PV parameters of PSC ($E_g = 1.52 \pm 0.3$ eV) over device active area of ~0.1 and 1 cm^2.[2,3,21–23] It is evident that J_{SC} and V_{OC} are not affected significantly by increasing the active area from 0.1 cm^2 to 1 cm^2, whereas the *FF* does, hence the device efficiency. This effect could be severe in further large area devices. It is of utmost importance to understand the loss in the *FF* due to increasing the device's active area to successfully fabricate scalable PSCs. Ho-Baillie and coworkers showed that the TCO substrate sheet resistance could influence the FF of large-area PSC devices apart from the non-uniform deposition of the device stack.[53] They fabricated *n-i-p* mesoscopic PSC device architecture on a conventional and U-shaped designed bottom gold electrode (150 nm thick) and showed certified efficiency of 19.63% with *FF* of 75.8% over an active area of 1.02 cm^2 [see Fig. 2(b)]. Depositing U-shaped electrodes on the TCO substrates enhances the electron collection efficiency in n-i-p device architecture. Figure 2(c) shows the simulated series resistance distribution for 10×10 mm^2 active area device, and it is lower for the U-shaped modified electrode, and the corresponding fill factor (*FF*) increased from 50.0% to 72.2%. The FF of the device also depends on the device geometry, as shown in Fig. 3(a). The series resistance is higher for the square-shaped electrode because the electrons travel a longer distance from the center, whereas it is lower for the strip-shaped electrode and shows an improved fill factor. However, the bottom electrode modification strategy is possible for the *n-i-p* device where the ETL (c-TiO_2 50 nm/mp-TiO_2 200 nm) thickness of ~250 nm could be deposited by spray pyrolysis/spin coating technique over 100–150 nm thick bottom U-shaped electrode. However, similar strategy is difficult to adopt in solution-processed *p-i-n* PSCs, as the HTL layer thickness is usually 2–3 nm of recently developed self-assembled monolayers (SAMs).[41,43,58] Such a 100–150 nm bottom U-shaped gold electrode would act as a barrier at the edges of the substrates and make it difficult to deposit uniform HTL using the solution-processed spin coating technique. Therefore, for a large area (≥ 1 cm^2) *p-i-n* device architecture, the U-shape electrode deposition is done (thermal evaporation or silver paste) after scratching the spin-coated thin film layers. Figures 3(b)–3(d) are the photographic images of large area (1 cm^2) PSCs using different electrode shapes. Unfortunately, most of the reports do not elaborate on the electrode design for large-area devices, which is a bad practice and lacks progress toward the scalability of PSCs. We believe reporting the device engineering, including electrode design, is required for successful scalable PSC fabrication. In addition, a systematic simulation or experimental study needs to be carried out to understand the series and shunt resistance losses for large-area devices to better understand the FF loss issues.

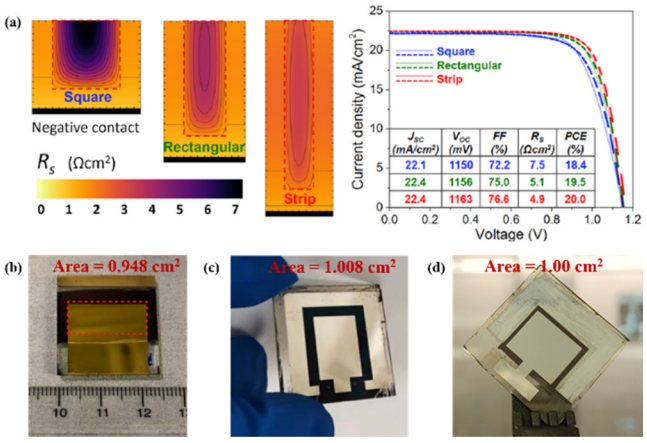

FIG. 3. (a) The left panel represents the simulated series resistance distributions for 10×10 mm^2, 6×17 mm^2, and 4×25 mm^2 devices using electrode designs with different geometries. The right panel shows the simulated (solid line) and measured (dashed line) $J - V$ curves of devices using new electrode designs with different geometries. Reprinted with permission from Ho-Baillie *et al.* Joule **2**, 2694 (2018). Copyright 2018 Elsevier Inc.[53] (b) Rectangular device active area of 0.948 cm^2 with one side TCO connection. Reprinted with permission from Yoo *et al.* Nature **590**, 587 (2021). Copyright 2021 Springer Nature.[59] (c) Rectangular device active area 1.008 cm^2 with four side TCO connection. Reprinted with permission from Fengzhu Li *et al.* Nat. Photonics **17**, 478 (2023). Copyright 2023 Springer Nature.[60] (d) Rectangular device active area 1.000 cm^2 with U-shaped (three side TCO connection) bottom electrode deposited after scribing the spin-coated layers.[61]

IV. STABILITY ANALYSIS OF PEROVSKITE SOLAR CELLS

To ensure the economic viability of perovskite technology, long-term stability is crucial apart from high efficiency and scalability. To compete with the market-leading commercialized PV technologies, the expected lifetime of the PV devices should be 20–25 years. It is impractical to use decade-long protocols for stability testing. Hence, accelerated aging tests are required to understand the lifetime span of PSCs. The stability of the PSCs depends on extrinsic (oxygen, moisture, and UV light exposure) and intrinsic (thermal and structural degradation, ion migration, and electrical bias) stresses. Extrinsic stress, such as oxygen-induced degradation, moisture degradation, and UV-light degradation, can be avoided by advanced encapsulation techniques. However, the intrinsic stability of the PSCs is a crucial factor, and understanding them and corresponding solutions need to be discussed for commercializing perovskite PV technology. Considering the material stability, the mixed organic-inorganic halide perovskites represented better choice for high efficiency and stable performance.[17,62] However, the existing accelerated aging tests described in an International Electrotechnical Commission (IEC) standards are used for testing the Si solar panel performance.[63] Unfortunately, these tests cannot be carried out in DSSC, OPV (organic PV), and PSCs as they are fundamentally different materials and PSCs also show ion migration, performance recovery in the dark conditions, etc., which are unknown in Si photovoltaics. In 2011, a consortium of researchers at the International Summit of Organic PV Stability developed standardized aging tests called ISOS protocols for testing the lab-scale OPV devices to ensure the comparability of PV testing performed at different laboratories.[64] Those protocols include the following stability testing standards: (i) dark storage (ISOS-D), (ii) light soaking (ISOS-L), (iii) outdoor stability (ISOS-O), (iv) thermal cycling (ISOS-T), (v) solar-thermal cycling (ISOS-LT), and each of which has three different levels determined by thermal stress, relative humidity stress, environment set-up, and light source and circuit bias (maximum power point tracking: MPPT or open circuit: OC). People reported different stability conditions and data formats in PSCs, preventing data comparison and identifying various degradation factors or failure mechanisms. The consensus statement in 2020 by Khenkin *et al.* proposes that the ISOS stability could be carried out in PSCs along with additional aging experiments such as (i) bias stability (ISOS-V) (ii) light cycling (ISOS-LC), and also reported a checklist that should be carried out for

reporting the stability of PSCs. The reason for adding bias stability and light cycling for PSC is discussed herein.

The ISOS-O-1 protocol suggests the periodic measurements of J–V curves under solar simulator light illumination in MPPT or OC bias conditions, whereas ISOS-O-2 requires natural sunlight. ISOS-O-3 requires both *in situ* MPPT under natural sunlight and periodic performance measurements under a solar simulator. Figure 4(a) shows the stability performance (ISOS-O) obtained by J–V measurements, and MPP tracking of PSCs do not coincide, although they generally have similar trends. Therefore, it is crucial when characterizing PSCs to describe the load and recovery time before each J–V measurement. The perovskite solar cell degradation mode is known to be reversible partly or entirely in the dark conditions, which is often referred to as metastability [see Fig. 4(b)]. Therefore, cycling through light-dark periods to mimic day-night cycles results in a significantly different stress test than applying constant illumination (ISOS-L). The improvement in the power conversion efficiency (PCE) under illumination after storage in the dark condition could be attributed to the passivation of interfacial defects by photogenerated charge carriers or ion migration induced modification of the built-in electric field.[65] However, the PCE dynamics during a cycle depend on the present status of cell degradation condition. Therefore, the ISOS protocols were revised for PSCs and included light–dark cycling protocols to account for the recovery phenomena (ISOS-LC). In addition, the electrical bias causes PSC degradation by stimulating the ion migration or charge carrier accumulation, resulting in thermally activated trap formation.[66] Therefore, ISOS protocols revisited for PSCs to include the ISOS-V, in which the behavior of the cell is analyzed when exposed to a certain electrical forward bias (maximum power point voltage:V_{MPP} or open circuit voltage: V_{OC} as measured in AM 1.5 G) in the dark [see Fig. 4(c)].

Interestingly, researchers also show additional degradation studies beyond ISOS protocols, such as exposure of PSCs using 10-sun illumination at the MPPT condition of the encapsulated devices [see Fig. 4(d)], and they show excellent thermal stability of $FA_{0.83}Cs_{0.17}PbI_{2.7}Br_{0.3}$ composition-based PSC.[62] When the 3D (three dimensional) perovskites come in contact with the environment (moisture, oxygen, or UV-light), they are subjected to severe degradation that limit the solar cell's lifetime. Different 2D (two dimensional) and quasi-2D perovskite materials demonstrated significant improvement in the efficiency and stability of 3D PSCs. The 2D perovskites exhibit multiple-quantum-well structures and offer tunable optoelectronic properties, defect passivation in the bulk and interface, superior thermal and light stability, hydrophobicity due to large organic cation, suppressing ion migration, etc.[68] To achieve simultaneously high efficiency and high stability for 3D PSCs using 2D perovskites, numerous device engineering strategy studies have been conducted, including compositional or additive engineering,

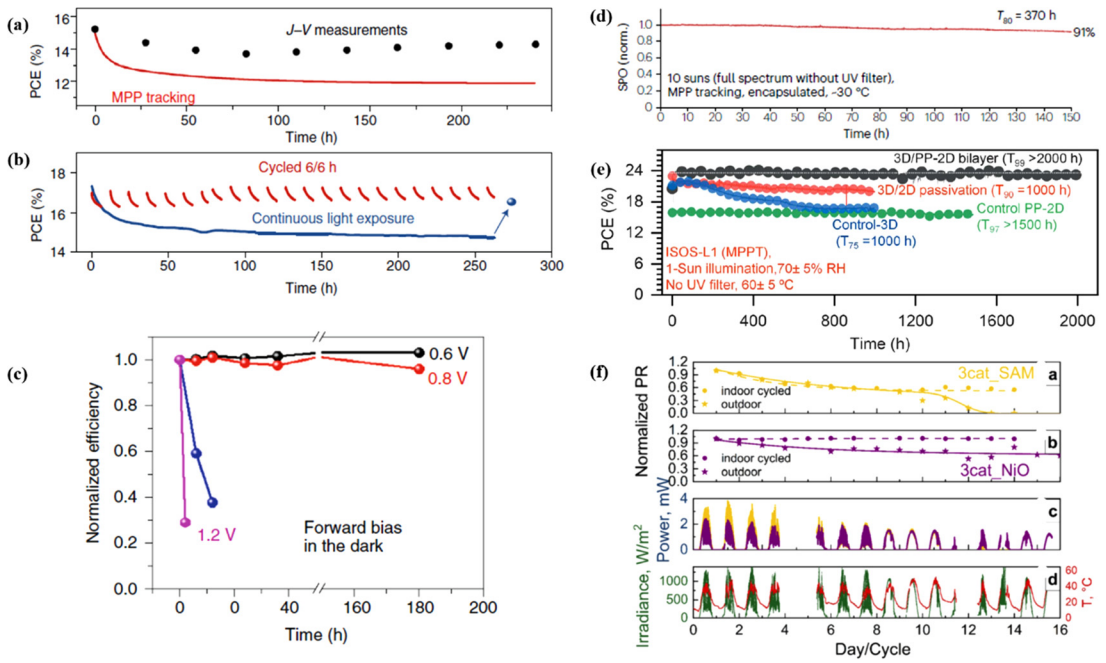

FIG. 4. (a) Power conversion efficiency (PCE) extracted from current density vs voltage ($J-V$) scans (black dots) and continuous MPP tracking (red curve) for the same PSC. Reprinted with permission from Khenkin *et al.* Nat. Energy **5**, 35 (2020). Copyright 2020 Springer Nature.[25] (b) PCE variation of PSCs upon continuous (blue curve) or cycled (6/6 h, red curves) illumination by white light emitting diodes. Reprinted with permission from Khenkin *et al.* Nat. Energy **5**, 35 (2020). Copyright 2020 Springer Nature.[25] (c) Normalized PCE of PSCs changes with forward bias in the dark condition. Reprinted with permission from Khenkin *et al.* Nat. Energy **5**, 35 (2020). Copyright 2020 Springer Nature.[25] (d) Stabilized power output (SPO) of the perovskite devices, continuously recorded under 10-sun concentration illumination. Reprinted with permission from Wang *et al.* Nat. Energy **3**(11), 1013 (2018). Copyright 2018 Springer Nature.[62] (e) ISOS-L-1 stability measured at MPPT in ambient condition under continuous 1-sun illumination (55 °C) for epoxy encapsulated control 3D and 2D passivated 3D PSC. Reprinted with permission from Sidhik *et al.* Science **377**(6613), 1425–1430 (2022). Copyright 2022 American Association for the Advancement of Science.[26] (f) Indoor cycled and outdoor stability of encapsulated PSCs with triple cation perovskite and different transport layers. The outdoor power output of the representative cells is depicted at the corresponding irradiance and temperature. Reprinted with permission from Khenkin *et al.* Energy Environ. Sci. **17**, 602 (2023). Copyright 2024 Royal Society of Chemistry.[67]

dimensional engineering, interfacial engineering, etc. Sum *et al.* used different 2D (and low dimensional) perovskite materials to passivate 3D perovskite surface defects and showed an efficiency of 24.1% with $T_{95} > 1000$ h at MPPT.[69] Wolf el. al. tailored the number of octahedral inorganic sheets in 2D perovskite passivation layers for 3D PSCs and showed an efficiency of 24.3% with $T_{95} > 1000$ h under damp heat testings (85 °C and RH 85%).[70] Mohite *et al.* carried out dimensional tunability and grew pure 2D phase perovskites of controlled thickness on the 3D perovskite layer using solvent engineering strategy and showed an efficiency of 24.5% with $T_{99} > 2000$ h under continuous 1-sun light at 55 °C and RH 65% [see Fig. 4(e)].[26] However, for the practical application of perovskite solar cells, the encapsulation of the PSC device is mandatory to prevent the penetration of oxygen, moisture, and lead leakage from the lead-based PSCs. Emery *et al.* recently performed the outdoor stability (ISOS-O3) of $FA_{0.85}Cs_{0.15}PbI_{2.55}Br_{0.45}$ composition-based PSC after encapsulation using glue-based epoxy and polyolefin elastomer (POE) + butyl lamination in a glass−glass stack.[71] They observed that the glue-based encapsulation lasts for only 3 months, whereas the POE-based encapsulation lasts for 10 months. However, the POE-based encapsulation is technically challenging to implement, but it provides excellent stability even under damp heat and outdoor test conditions. The POE + butyl lamination in a glass–glass stack of PSC restricts its use as it requires an annealing temperature of 150 °C for 20 min for the lamination process, which could damage the methylammonium iodide (MAI) containing perovskites. Therefore, developing encapsulation technology for perovskite solar cells is of utmost importance for commercialization of it. Nevertheless, it is crucial to understand that the indoor stability test results as per ISOS protocols do not match the outdoor stability results due to the transient behavior of PSCs not being accounted for in the standard ISOS constant illumination testing conditions. Abate *et al.* showed that light cycling shows much better agreement with outdoor observations, at least qualitative (and even quantitative in some cases), as shown in Fig. 4(f). Apart from all these different accelerated aging tests, the important question is how can we predict the practical lifetime of the PSCs from these aging tests. As far as we know, no methods have been developed yet to estimate the practical lifetime from these accelerated tests for PSCs. So, to speed up the commercialization of PSCs, it is of utmost importance to develop a simulation model to predict the real field lifetime of the PSCs using the accelerated aging test results. However, Solar Energy Technologies Office (SETO) in DOE, USA, and Perovskite PV Accelerator for Commercializing Technology (PACT) have made a joint effort to perform the field deployment testing. PACT has planned to develop standardized testing protocols to establish outdoor testing to ensure their accelerated aging tests accurately reproduce the real field degradation mechanisms and allow researchers to corroborate their prototypes in the real field.[72]

V. CONCLUSIONS AND OUTLOOK

The efficiency number reported on the PSCs over active area <0.1 to 1 cm^2 is comparable to the commercialized Si solar cells. However, significant efforts are required to improve the scalability and stability of PSCs. For tandem cells, wider bandgap cells are being developed; however, the wide bandgap perovskites show losses in V_{OC} due to band offset apart from bulk and non-radiative defects. This requires good band alignment of the HTL/perovskite interface. Therefore, deeper HOMO level-based HTLs need to be developed. The scalability is a challenge in PSCs because of *FF* loss in the large area devices mainly due to sheet resistance limitation. Therefore, researchers need to focus on device engineering, including electrode design. The accelerated aging test of the PSCs requires more attention, and outdoor field experiments must be performed to understand the real field degradation and failure mechanism. To improve the life span of the PSC device, dedicated research is required for the development of the encapsulation technology. It is impractical to use decade-long protocols for stability testing; hence, it is of utmost importance to develop a simulation model to predict the real field lifetime of the PSCs using the accelerated aging test results.

ACKNOWLEDGMENTS

K.H. acknowledges MoE-India for the I-PDF IIT Bombay fellowship, and S.N. acknowledges the Ministry of Human Resource Development, India, for the doctoral fellowship. This work was supported by the Ministry of New and Renewable Energy India: National Centre for Photovoltaic Research and Education (NCPRE) Phase III. This work was also partially supported by a DST-Solar Challenge Award (No. DST/ETC/CASE/RES/2023/02). D.K. also acknowledges Forbes Marshall financial support for the Energy Science and Engineering chair professorship. We acknowledge Johns Aji for his help in making the TOC figure.

AUTHOR DECLARATIONS

Conflict of Interest

The authors have no conflicts to disclose.

Author Contributions

Kashimul Hossain: Conceptualization (equal); Data curation (equal); Writing – original draft (lead). **Suryanarayan Nayak:** Data curation (supporting); Writing – original draft (supporting); Writing – review & editing (supporting). **Dinesh Kabra:** Conceptualization (equal); Data curation (equal); Funding acquisition (lead); Project administration (lead); Supervision (lead); Writing – review & editing (equal).

DATA AVAILABILITY

Data sharing is not applicable to this article as no new data were created or analyzed in this study.

REFERENCES

[1]A. Kojima, K. Teshima, Y. Shirai, and T. Miyasaka, "Organometal halide perovskites as visible-light sensitizers for photovoltaic cells," J. Am. Chem. Soc. **131**(17), 6050–6051 (2009).
[2]J. Zhou, L. Tan, Y. Liu, H. Li, X. Liu, M. Li, S. Wang, Y. Zhang, C. Jiang, R. Hua, W. Tress, S. Meloni, and C. Yi, "Highly efficient and stable perovskite solar cells via a multifunctional hole transporting material," Joule **8**(6), 1691–1706 (2024).
[3]Z. Liang, Y. Zhang, H. Xu, W. Chen, B. Liu, J. Zhang, H. Zhang, Z. Wang, D. H. Kang, J. Zeng, X. Gao, Q. Wang, H. Hu, H. Zhou, X. Cai, X. Tian, P. Reiss, B. Xu, T. Kirchartz, Z. Xiao, S. Dai, N. G. Park, J. Ye, and X. Pan, "Homogenizing out-of-plane cation composition in perovskite solar cells," Nature **624**(7992), 557–563 (2023).
[4]K. Hossain, D. Sivadas, D. Kabra, and P. R. Nair, "Perovskite solar cells dominated by bimolecular recombination—How far is the radiative limit?," ACS Energy Lett. **9**(5), 2310–2317 (2024).
[5]S. Sidhik, I. Metcalf, W. Li, T. Kodalle, C. J. Dolan, M. Khalili, J. Hou, F. Mandani, A. Torma, H. Zhang, R. Garai, J. Persaud, A. Marciel, I. A. Muro Puente, G. N. M. Reddy, A. Balvanz, M. A. Alam, C. Katan, E. Tsai, D. Ginger,

D. P. Fenning, M. G. Kanatzidis, C. M. Sutter-Fella, J. Even, and A. D. Mohite, "Two-dimensional perovskite templates for durable, efficient formamidinium perovskite solar cells," Science **384**(6701), 1227–1235 (2024).
[6]Y. Shi, J. J. Berry, and F. Zhang, "Perovskite/silicon tandem solar cells: Insights and outlooks," ACS Energy Lett. **9**(3), 1305–1330 (2024).
[7]S. Singh, Laxmi, and D. Kabra, "Defects in halide perovskite semiconductors: Impact on photo-physics and solar cell performance," J. Phys. D: Appl. Phys. **53**(50), 503003 (2020).
[8]A. Miyata, A. Mitioglu, P. Plochocka, O. Portugall, J. T. W. Wang, S. D. Stranks, H. J. Snaith, and R. J. Nicholas, "Direct measurement of the exciton binding energy and effective masses for charge carriers in organic-inorganic tri-halide perovskites," Nat. Phys. **11**(7), 582–587 (2015).
[9]J. S. Manser, J. A. Christians, and P. V. Kamat, "Intriguing optoelectronic properties of metal halide perovskites," Chem. Rev. **116**(21), 12956–13008 (2016).
[10]G. Kim and A. Petrozza, "Defect tolerance and intolerance in metal-halide perovskites," Adv. Energy Mater. **10**(37), 2001959 (2020).
[11]M. H. White and J. R. Cricchi, "Characterization of thin-oxide MNOS memory transistors," IEEE Trans. Electron Devices **19**(12), 1280–1288 (1972).
[12]J. J. Yoo, S. S. Shin, and J. Seo, "Toward efficient perovskite solar cells: Progress, strategies, and perspectives," ACS Energy Lett. **7**(6), 2084–2091 (2022).
[13]L. Meng, J. You, and Y. Yang, "Addressing the stability issue of perovskite solar cells for commercial applications," Nat. Commun. **9**(1), 5265 (2018).
[14]T. D. Siegler, A. Dawson, P. Lobaccaro, D. Ung, M. E. Beck, G. Nilsen, and L. L. Tinker, "Erratum: The path to perovskite commercialization: A perspective from the United States solar energy technologies office [ACS Energy Lett. **7**(5), 1728–1734 (2022)]," ACS Energy Lett. **7**, 2113 (2022).
[15]E. J. Juarez-Perez, L. K. Ono, and Y. Qi, "Thermal degradation of formamidinium based lead halide perovskites into: Sym-triazine and hydrogen cyanide observed by coupled thermogravimetry-mass spectrometry analysis," J. Mater. Chem. A **7**(28), 16912–16919 (2019).
[16]K. Hossain, S. Singh, and D. Kabra, "Role of monovalent cations in the dielectric relaxation processes in hybrid metal halide perovskite solar cells," ACS Appl. Energy Mater. **5**(3), 3689–3697 (2022).
[17]M. Saliba, T. Matsui, J. Y. Seo, K. Domanski, J. P. Correa-Baena, M. K. Nazeeruddin, S. M. Zakeeruddin, W. Tress, A. Abate, A. Hagfeldt, and M. Grätzel, "Cesium-containing triple cation perovskite solar cells: Improved stability, reproducibility and high efficiency," Energy Environ. Sci. **9**(6), 1989–1997 (2016).
[18]H. Lu, A. Krishna, S. M. Zakeeruddin, M. Grätzel, and A. Hagfeldt, "Compositional and interface engineering of organic-inorganic lead halide perovskite solar cells," IScience **23**(8), 101359 (2020).
[19]A. Rajagopal, Z. Yang, S. B. Jo, I. L. Braly, P. W. Liang, H. W. Hillhouse, and A. K. Y. Jen, "Highly efficient perovskite–perovskite tandem solar cells reaching 80% of the theoretical limit in photovoltage," Adv. Mater. **29**(34), 1702140 (2017).
[20]A. Paul, A. Singha, K. Hossain, S. Gupta, M. Misra, S. Mallick, A. H. Munshi, and D. Kabra, "4-T CdTe/perovskite thin film tandem solar cells with efficiency> 24%," ACS Energy Lett. **9**, 3019–3026 (2024).
[21]M. Jeong, I. W. Choi, E. M. Go, Y. Cho, M. Kim, B. Lee, S. Jeong, Y. Jo, H. W. Choi, J. Lee, J. H. Bae, S. K. Kwak, D. S. Kim, and C. Yang, "Stable perovskite solar cells with efficiency exceeding 24.8% and 0.3-V voltage loss," Science **369**(6511), 1615–1620 (2020).
[22]G. Li, Z. Su, L. Canil, D. Hughes, M. H. Aldamasy, J. Dagar, S. Trofimov, L. Wang, W. Zuo, J. J. Jerónimo-Rendon, M. M. Byranvand, C. Wang, R. Zhu, Z. Zhang, F. Yang, G. Nasti, B. Naydenov, W. C. Tsoi, Z. Li, X. Gao, Z. Wang, Y. Jia, E. Unger, M. Saliba, M. Li, and A. Abate, "Highly efficient p-i-n perovskite solar cells that endure temperature variations," Science **379**(6630), 399–403 (2023).
[23]W. Peng, K. Mao, F. Cai, H. Meng, Z. Zhu, T. Li, S. Yuan, Z. Xu, X. Feng, J. Xu, M. D. McGehee, and J. Xu, "Reducing nonradiative recombination in perovskite solar cells with a porous insulator contact," Science **379**(6633), 683–690 (2023).
[24]T. Wu, Z. Qin, Y. Wang, Y. Wu, W. Chen, S. Zhang, M. Cai, S. Dai, J. Zhang, J. Liu, Z. Zhou, X. Liu, H. Segawa, H. Tan, Q. Tang, J. Fang, Y. Li, L. Ding, Z. Ning, Y. Qi, Y. Zhang, and L. Han, "The main progress of perovskite solar cells in 2020–2021," Nano-Micro Lett. **13**(1), 1–18 (2021).
[25]M. V. Khenkin, E. A. Katz, A. Abate, G. Bardizza, J. J. Berry, C. Brabec, F. Brunetti, V. Bulović, Q. Burlingame, A. Di Carlo, R. Cheacharoen, Y. B. Cheng, A. Colsmann, S. Cros, K. Domanski, M. Dusza, C. J. Fell, S. R. Forrest, Y. Galagan, D. Di Girolamo, M. Grätzel, A. Hagfeldt, E. von Hauff, H. Hoppe, J. Kettle, H. Köbler, M. S. Leite, S. (Frank) Liu, Y. L. Loo, J. M. Luther, C. Q. Ma, M. Madsen, M. Manceau, M. Matheron, M. McGehee, R. Meitzner, M. K. Nazeeruddin, A. F. Nogueira, Ç. Odabaşı, A. Osherov, N. G. Park, M. O. Reese, F. De Rossi, M. Saliba, U. S. Schubert, H. J. Snaith, S. D. Stranks, W. Tress, P. A. Troshin, V. Turkovic, S. Veenstra, I. Visoly-Fisher, A. Walsh, T. Watson, H. Xie, R. Yıldırım, S. M. Zakeeruddin, K. Zhu, and M. Lira-Cantu, "Consensus statement for stability assessment and reporting for perovskite photovoltaics based on ISOS procedures," Nat. Energy **5**(1), 35–49 (2020).
[26]S. Sidhik, Y. Wang, M. De Siena, R. Asadpour, A. J. Torma, T. Terlier, K. Ho, W. Li, A. B. Puthirath, X. Shuai, A. Agrawal, B. Traore, M. Jones, R. Giridharagopal, P. M. Ajayan, J. Strzalka, D. S. Ginger, C. Katan, M. A. Alam, J. Even, M. G. Kanatzidis, and A. D. Mohite, "Deterministic fabrication of 3D/2D perovskite bilayer stacks for durable and efficient solar cells," Science **377**(6613), 1425–1430 (2022).
[27]pv magazine, see https://www.pv-magazine.com/2022/02/18/chinese-pv-industry-brief-microquanta-builds-12-mw-ground-mounted-project-with-perovskite-solar-modules/ for "Bridge to a sustainable future" (n.d.).
[28]SOLARBE GLOBAL, see https://www.solarbeglobal.com/top-10-perovskite-solar-module-companies-in-china/#:~:text=9.,of%20large%2Dscale%20cell%20modules for "Top 10 perovskite solar module companies in China" (n.d.).
[29]Perovskite-info, see https://www.perovskite-info.com/kunshan-gcl-photoelectric-materials-announces-1904-efficiency-single-junction for "Kunshan GCL photoelectric materials announces 19.04% efficiency on single-junction perovskite modules (1000 mm × 2000 mm)" (n.d.).
[30]Z. Li, Y. Zhao, X. Wang, Y. Sun, Z. Zhao, Y. Li, H. Zhou, and Q. Chen, "Cost analysis of perovskite tandem photovoltaics," Joule **2**(8), 1559–1572 (2018).
[31]M. Johnsson and P. Lemmens, "Perovskites and thin films - crystallography and chemistry," J. Phys. Condens. Matter **20**(26), 264001 (2008).
[32]J. Seo, T. Song, S. Rasool, S. Park, and J. Y. Kim, "An overview of lead, tin, and mixed tin–lead-based ABI3 perovskite solar cells," Adv. Energy Sustainable Res. **4**(5), 2200160 (2023).
[33]N. Liu and C. Y. Yam, "First-principles study of intrinsic defects in formamidinium lead triiodide perovskite solar cell absorbers," Phys. Chem. Chem. Phys. **20**(10), 6800–6804 (2018).
[34]E. M. Hutter, L. A. Muscarella, F. Wittmann, J. Versluis, L. McGovern, H. J. Bakker, Y. W. Woo, Y. K. Jung, A. Walsh, and B. Ehrler, "Thermodynamic stabilization of mixed-halide perovskites against phase segregation," Cell Rep. Phys. Sci. **1**(8), 100120 (2020).
[35]S. Rühle, "Tabulated values of the Shockley-Queisser limit for single junction solar cells," Sol. Energy **130**, 139–147 (2016).
[36]E. Aydin, T. G. Allen, M. De Bastiani, L. Xu, J. Ávila, M. Salvador, E. Van Kerschaver, and S. De Wolf, "Interplay between temperature and bandgap energies on the outdoor performance of perovskite/silicon tandem solar cells," Nat. Energy **5**(11), 851–859 (2020).
[37]M. R. Filip, G. E. Eperon, H. J. Snaith, and F. Giustino, "Steric engineering of metal-halide perovskites with tunable optical band gaps," Nat. Commun. **5**(1), 5757 (2014).
[38]J. Jeong, M. Kim, J. Seo, H. Lu, P. Ahlawat, A. Mishra, Y. Yang, M. A. Hope, F. T. Eickemeyer, M. Kim, Y. J. Yoon, I. W. Choi, B. P. Darwich, S. J. Choi, Y. Jo, J. H. Lee, B. Walker, S. M. Zakeeruddin, L. Emsley, U. Rothlisberger, A. Hagfeldt, D. S. Kim, M. Grätzel, and J. Y. Kim, "Pseudo-halide anion engineering for α-FAPbI3 perovskite solar cells," Nature **592**(7854), 381–385 (2021).
[39]Y. Jin, H. Feng, Z. Fang, H. Zhang, L. Yang, X. Chen, Y. Li, B. Deng, Y. Zhong, Q. Zeng, J. Huang, Y. Weng, J. Yang, C. Tian, L. Xie, J. Zhang, and Z. Wei, "Efficient and stable monolithic perovskite/silicon tandem solar cells enabled by contact-resistance-tunable indium tin oxide interlayer," Adv. Mater. **36**(35), 2404010 (2024).
[40]W. Zia, M. Malekshahi Byranvand, T. Rudolph, M. Rai, M. Kot, C. Das, M. Kedia, M. Zohdi, W. Zuo, V. Yeddu, M. I. Saidaminov, J. I. Flege, T. Kirchartz, and M. Saliba, "MAPbCl3 light absorber for highest voltage perovskite solar cells," ACS Energy Lett. **9**(3), 1017–1024 (2024).
[41]K. Hossain, A. Kulkarni, U. Bothra, B. Klingebiel, T. Kirchartz, M. Saliba, and D. Kabra, "Resolving the hydrophobicity of the Me-4PACz hole transport layer for inverted perovskite solar cells with efficiency >20%," ACS Energy Lett. **8**(9), 3860–3867 (2023).

[42]F. Penã-Camargo, P. Caprioglio, F. Zu, E. Gutierrez-Partida, C. M. Wolff, K. Brinkmann, S. Albrecht, T. Riedl, N. Koch, D. Neher, and M. Stolterfoht, "Halide segregation versus interfacial recombination in bromide-rich wide-gap perovskite solar cells," ACS Energy Lett. **5**(8), 2728–2736 (2020).
[43]I. Levine, A. Al-Ashouri, A. Musiienko, H. Hempel, A. Magomedov, A. Drevilkauskaite, V. Getautis, D. Menzel, K. Hinrichs, T. Unold, S. Albrecht, and T. Dittrich, "Charge transfer rates and electron trapping at buried interfaces of perovskite solar cells," Joule **5**(11), 2915–2933 (2021).
[44]The Perovskite database, see https://www.perovskitedatabase.com/ for "The Perovskite database project" (n.d.).
[45]P. K. Nayak, S. Mahesh, H. J. Snaith, and D. Cahen, "Photovoltaic solar cell technologies: Analysing the state of the art," Nat. Rev. Mater. **4**(4), 269–285 (2019).
[46]L. V. Torres Merino, C. E. Petoukhoff, O. Matiash, A. S. Subbiah, C. V. Franco, P. Dally, B. Vishal, S. Kosar, D. Rosas Villalva, V. Hnapovskyi, E. Ugur, S. Shah, F. Peña Camargo, O. Karalis, H. Hempel, I. Levine, R. R. Pradhan, S. Kralj, N. Kalasariya, M. Babics, B. K. Yildirim, A. A. Said, E. Aydin, H. Bristow, S. Mannar, W. Raja, A. R. Pininti, A. Prasetio, A. Razzaq, H. Al Nasser, T. G. Allen, F. H. Isikgor, D. Baran, T. D. Anthopoulos, M. M. Masis, U. Schwingenschlögl, T. Unold, M. Stolterfoht, F. Laquai, and S. De Wolf, "Impact of the valence band energy alignment at the hole-collecting interface on the photostability of wide band-gap perovskite solar cells," Joule **8**, 2585 (2024).
[47]LIST SOLAR, see https://list.solar/news/kunshan-gcl-achieves/ for "Kunshan GCL achieves record 19.04% efficiency on perovskite modules" (n.d.).
[48]K. Hossain, B. Bhardwaj, and D. Kabra, "Low dark current with high-speed detection in a scalable perovskite photodetector," Device **0**, 100513 (2024); available at https://www.cell.com/action/showCitFormats?doi=10.1016%2Fj.device.2024.100513&pii=S2666-9986%2824%2900413-7.
[49]D. A. Chalkias, A. Mourtzikou, G. Katsagounos, A. N. Kalarakis, and E. Stathatos, "Development of greener and stable inkjet-printable perovskite precursor inks for all-printed annealing-free perovskite solar mini-modules manufacturing," Small Methods **7**(10), 2300664 (2023).
[50]X. Zhao, P. Zhang, T. Liu, B. Tian, Y. Jiang, J. Zhang, Y. Tang, B. Li, M. Xue, W. Zhang, Z. Zhang, and W. Guo, "Operationally stable perovskite solar modules enabled by vapor-phase fluoride treatment," Science **385**(6707), 433–438 (2024).
[51]C. Yang, W. Hu, J. Liu, C. Han, Q. Gao, A. Mei, Y. Zhou, F. Guo, and H. Han, "Achievements, challenges, and future prospects for industrialization of perovskite solar cells," Light. Sci. Appl. **13**(1), 227 (2024).
[52]F. H. Isikgor, A. S. Subbiah, M. K. Eswaran, C. T. Howells, A. Babayigit, M. De Bastiani, E. Yengel, J. Liu, F. Furlan, G. T. Harrison, S. Zhumagali, J. I. Khan, F. Laquai, T. D. Anthopoulos, I. McCulloch, U. Schwingenschlögl, and S. De Wolf, "Scaling-up perovskite solar cells on hydrophobic surfaces," Nano Energy **81**, 105633 (2021).
[53]M. Zhang, B. Wilkinson, Y. Liao, J. Zheng, C. F. J. Lau, J. Kim, J. Bing, M. A. Green, S. Huang, and A. W. Y. Ho-Baillie, "Electrode design to overcome substrate transparency limitations for highly efficient 1 cm^2 mesoscopic perovskite solar cells," Joule **2**(12), 2694–2705 (2018).
[54]M. Saliba, E. Unger, L. Etgar, J. Luo, and T. J. Jacobsson, "A systematic discrepancy between the short circuit current and the integrated quantum efficiency in perovskite solar cells," Nat. Commun. **14**(1), 5445 (2023).
[55]S. Singh, R. J. Shourie, and D. Kabra, "Efficient and thermally stable CH3NH3PbI3 based perovskite solar cells with double electron and hole extraction layers," J. Phys. D: Appl. Phys. **52**(25), 255106 (2019).
[56]M. Saliba and L. Etgar, "Current density mismatch in Perovskite solar cells," ACS Energy Lett. **5**(9), 2886–2888 (2020).
[57]X. Xu, J. Shi, H. Wu, Y. Yang, J. Xiao, Y. Luo, D. Li, and Q. Meng, "The influence of different mask aperture on the open-circuit voltage measurement of perovskite solar cells," J. Renewable Sustainable Energy **7**(4), 043104 (2015).
[58]N. Gaur, M. Misra, K. Hossain, and D. Kabra, "Improved thermally activated delayed fluorescence-based electroluminescent devices using vacuum-processed carbazole-based self-assembled monolayers," ACS Energy Lett. **9**(3), 1056–1062 (2024).
[59]J. J. Yoo, G. Seo, M. R. Chua, T. G. Park, Y. Lu, F. Rotermund, Y. K. Kim, C. S. Moon, N. J. Jeon, J. P. Correa-Baena, V. Bulović, S. S. Shin, M. G. Bawendi, and J. Seo, "Efficient perovskite solar cells via improved carrier management," Nature **590**(7847), 587–593 (2021).
[60]F. Li, X. Deng, Z. Shi, S. Wu, Z. Zeng, D. Wang, Y. Li, F. Qi, Z. Zhang, Z. Yang, S. H. Jang, F. R. Lin, S. -W. Tsang, X. K. Chen, and A. K. Y. Jen, "Hydrogen-bond-bridged intermediate for perovskite solar cells with enhanced efficiency and stability," Nat. Photonics **17**(6), 478–484 (2023).
[61]pv magazine, see https://www.pv-magazine.com/2024/02/22/inverted-perovskite-solar-cell-with-antimony-doped-tin-oxides-achieves-25-7-efficiency/ for "Inverted perovskite solar cell with antimony-doped tin oxides achieves 25.7% efficiency" (n.d.).
[62]Z. Wang, Q. Lin, B. Wenger, M. G. Christoforo, Y. H. Lin, M. T. Klug, M. B. Johnston, L. M. Herz, and H. J. Snaith, "Erratum to: High irradiance performance of metal halide perovskites for concentrator photovoltaics (Nature Energy, (2018), 3, 10, (855–861), 10.1038/s41560-018–0220-2)," Nat. Energy **3**(11), 1013 (2018).
[63]IEC Webstore, see https://webstore.iec.ch/en/publication/24312 for "IEC 61215–1:2016 terrestrial photovoltaic (pv) modules - design qualification and type approval - Part 1: Test Requirements" (2016).
[64]M. O. Reese, S. A. Gevorgyan, M. Jørgensen, E. Bundgaard, S. R. Kurtz, D. S. Ginley, D. C. Olson, M. T. Lloyd, P. Morvillo, E. A. Katz, A. Elschner, O. Haillant, T. R. Currier, V. Shrotriya, M. Hermenau, M. Riede, K. R. Kirov, G. Trimmel, T. Rath, O. Inganäs, F. Zhang, M. Andersson, K. Tvingstedt, M. Lira-Cantu, D. Laird, C. McGuiness, S. Gowrisanker, M. Pannone, M. Xiao, J. Hauch, R. Steim, D. M. Delongchamp, R. Rösch, H. Hoppe, N. Espinosa, A. Urbina, G. Yaman-Uzunoglu, J. B. Bonekamp, A. J. J. M. Van Breemen, C. Girotto, E. Voroshazi, and F. C. Krebs, "Consensus stability testing protocols for organic photovoltaic materials and devices," Sol. Energy Mater. Sol. Cells **95**(5), 1253–1267 (2011).
[65]C. Zhao, B. Chen, X. Qiao, L. Luan, K. Lu, and B. Hu, "Revealing underlying processes involved in light soaking effects and hysteresis phenomena in perovskite solar cells," Adv. Energy Mater. **5**(14), 1500279 (2015).
[66]B. Chen, J. Song, X. Dai, Y. Liu, P. N. Rudd, X. Hong, and J. Huang, "Synergistic effect of elevated device temperature and excess charge carriers on the rapid light-induced degradation of perovskite solar cells," Adv. Mater. **31**(35), 1902413 (2019).
[67]M. Khenkin, H. Köbler, M. Remec, R. Roy, U. Erdil, J. Li, N. Phung, G. Adwan, G. Paramasivam, Q. Emery, E. Unger, R. Schlatmann, C. Ulbrich, and A. Abate, "Light cycling as a key to understanding the outdoor behaviour of perovskite solar cells," Energy Environ. Sci. **17**(2), 602–610 (2024).
[68]W. Chi and S. K. Banerjee, "Engineering strategies for two-dimensional perovskite solar cells," Trends Chem. **4**(11), 1005–1020 (2022).
[69]S. Ye, H. Rao, M. Feng, L. Xi, Z. Yen, D. H. L. Seng, Q. Xu, C. Boothroyd, B. Chen, Y. Guo, B. Wang, T. Salim, Q. Zhang, H. He, Y. Wang, X. Xiao, Y. M. Lam, and T. C. Sum, "Expanding the low-dimensional interface engineering toolbox for efficient perovskite solar cells," Nat. Energy **8**(3), 284–293 (2023).
[70]R. Azmi, E. Ugur, A. Seitkhan, F. Aljamaan, A. S. Subbiah, J. Liu, G. T. Harrison, M. I. Nugraha, M. K. Eswaran, and M. Babics, "Damp heat–stable perovskite solar cells with tailored-dimensionality 2D/3D heterojunctions," Science **376**(6588), 73–77 (2022).
[71]Q. Emery, M. Remec, G. Paramasivam, S. Janke, J. Dagar, C. Ulbrich, R. Schlatmann, B. Stannowski, E. Unger, and M. Khenkin, "Encapsulation and outdoor testing of perovskite solar cells: Comparing industrially relevant process with a simplified lab procedure," ACS Appl. Mater. Interfaces **14**(4), 5159–5167 (2022).
[72]Sandia National Laboratories, see https://pvpact.sandia.gov/ for "Perovskite PV accelerator for commercializing technologies" (n.d.).